

# Algorithms Trained on Normal Chest X-rays Can Predict Health Insurance Types

**Chi-Yu Chen**

*National Taiwan University Hospital, Taiwan*

ALTIS5526@GMAIL.COM

**Rawan Abulibdeh**\*

*University of Toronto, Canada*

RAWAN.ABULIBDEH@MAIL.UTORONTO.CA

**Arash Asgari**\*

*York University, Canada*

ARASH.ASGARI.M@GMAIL.COM

**Leo Anthony Celi**\*

*Massachusetts Institute of Technology, USA*

LCELI@MIT.EDU

**Deirdre Goode**\*

*Mass General Brigham, USA*

DGOODE1@MGB.ORG

**Hassan Hamidi**\*

*York University, Canada*

HHAMIDI.HE@GMAIL.COM

**Laleh Seyyed-Kalantari**\*

*York University, Canada*

LSK@YORKU.CA

**Po-Chih Kuo**\*

*National Tsing Hua University, Taiwan*

KUOPC@CS.NTHU.EDU.TW

**Ned McCague**\*

*MIT, USA*

NMCCAGUE@MIT.EDU

**Thomas Sounack**\*

*Dana-Farber Cancer Institute, USA*

THOMAS\_SOUNACK@DFCI.HARVARD.EDU

## Abstract

Artificial intelligence is revealing what medicine never intended to encode. Deep vision models, trained on chest X-rays, can now detect not only disease but also invisible traces of social inequality. In this study, we show that state-of-the-art architectures (DenseNet121, SwinV2-B\*, MedMamba) can predict a patient’s health insurance type, a strong proxy for socioeconomic status, from normal chest X-rays with significant accuracy (AUC  $\approx$  0.67 on MIMIC-CXR-JPG, 0.68 on CheXpert). The signal persists even when age, race, and sex are controlled for, and remains detectable when the model is trained exclusively on a single racial group. Patch-based occlusion reveals that the signal is diffuse rather than localized, embedded in the upper and mid-thoracic regions. This suggests that deep networks may be internaliz-

ing subtle traces of clinical environments, equipment differences, or care pathways; learning socioeconomic segregation itself. These findings challenge the assumption that medical images are neutral biological data. By uncovering how models perceive and exploit these hidden social signatures, this work reframes fairness in medical AI: the goal is no longer only to balance datasets or adjust thresholds, but to interrogate and disentangle the social fingerprints embedded in clinical data itself.

**Keywords:** spurious correlation, health insurance, medical images

**Data and Code Availability** The code is published on [code](#).

**Institutional Review Board (IRB)** IRB approval is not required in our study

\* These authors contributed equally to this work; author names are placed in alphabetical order by last name.

## 1. Introduction

Artificial intelligence (AI) has become increasingly part of our everyday life. However, experts acknowledge concerns regarding AI fairness, specifically the disparate outcomes of an AI model across different societal subpopulations [Seyyed-Kalantari et al. \(2020\)](#). Such considerations are paramount given that the outcomes of AI-facilitated decision-making are directly correlated with an individual’s well-being. Recent studies [Geirhos et al. \(2020\)](#); [Kim et al. \(2019\)](#); [Buolamwini and Gebru \(2018\)](#) have demonstrated that deep learning methods are prone to exploit spurious correlation from shortcut features, which are predictive features that do not correspond to disease-specific patterns [Banerjee et al. \(2023\)](#). The data distribution may also be polluted by multiple political, historical, or socioeconomic factors that exist in human society, containing unethical information that could be realized by AI algorithms and used by them. For example, [Obermeyer et al. \(2019\)](#) showed that a widely used commercial health prediction system treated different racial groups unequally since black patients were likely to spend less on healthcare than white patients, which might be correlated to hindered access to healthcare facilities for black patients. Therefore, researchers have been investigating the equality of AI algorithms treating people with different demographic data attributes (such as sex, race, age) across various modalities. [Larrazabal et al. \(2020\)](#); [Kumar et al. \(2025\)](#).

While shortcut features could be obvious and easy to identify, such as chest tube or watermarks on a medical image; we are more concerned with those that are imperceptible and unidentifiable to humans, such as demographic information in a chest X-ray. Demographic information could even introduce significant societal bias if they act as a shortcut feature. A leading study [Gichoya et al. \(2022\)](#) showed that the race of patients is strongly detectable from chest X-rays and other studies localized race features on medical images to highlight how AI detect race from chest X-rays [Konate et al. \(2025\)](#); [Salvado et al. \(2024\)](#). [Adleberg et al. \(2022\)](#) discussed the hidden health insurance information in the chest X-ray images. However, the study included patients of all ages in MIMIC-IV, overlooking the fact that people older than 65 are automatically enrolled in public insurance. Moreover, they did not exclude the chest X-rays with thoracic diseases, which is another confounding factor of health insurance status.

In this finding paper, we demonstrated the potential of AI algorithms to detect health insurance types from chest X-ray images. The lower performance of AI model in Chest X-ray disease diagnosis [Seyyed-Kalantari et al. \(2020\)](#) for low income patients with public insurance and the underdiagnosis bias against those patients has been documented in [Seyyed-Kalantari et al. \(2021, 2020\)](#); [Bahre et al. \(2025\)](#), necessitating further investigation to validate the presence of health insurance information within chest X-ray images. Therefore, our contribution is as below:

1. To the best of our knowledge, this is the first in-depth analysis that reveals that deep vision models (DenseNet [Huang et al. \(2017\)](#), SwinTransformer [Liu et al. \(2022\)](#), MedMamba [Yue and Li \(2024\)](#)) can predict health insurance types from normal chest X-ray images (without thoracic diseases) in the MIMIC-CXR-JPG and CheXpert dataset. This suggests that chest X-rays (CXRs) contain latent socioeconomic information about patients that AI models can potentially leverage.
2. We localized health insurance type information in chest X-ray images and demonstrated that there is likely more information in the upper two-third part of a chest X-ray.
3. From close analysis between health insurance types and other demographic features (e.g. age, race, sex), we found that these common demographic features do not act as an essential mediator in our insurance type prediction task, which indicates that the deep vision models directly detect insurance type signals from chest X-ray images.

## 2. Methods

### 2.1. Datasets

In our experiment, two medical datasets were utilized: MIMIC-CXR-JPG [Johnson et al. \(2019a,b\)](#) and CheXpert [Irvin et al. \(2019\)](#). MIMIC-CXR-JPG is an extended image dataset for MIMIC-IV v3.0 [Johnson et al. \(2024, 2023\)](#), including 377,110 chest X-ray images in total. We utilized MIMIC-CXR-JPG and linked it to MIMIC-IV v3.0 data by subject ID to attain patients’ health insurance type. There are six health insurance categories in MIMIC-IV v3.0: Medicaid, Medicare, Private, Self-pay, No

charge, and Other. On the other hand, CheXpert includes 224,316 chest X-rays from 65,240 patients from centers of Stanford Hospital. The recent CheXpert Plus paper [Chambon et al. \(2024\)](#) provides additional health insurance information for each patient, in which there are three categories: Medicaid, Medicare, and Private. As for CheXpert, we utilized the JPG-downsized version due to computational limits. (See appendix A for detailed description.) For both datasets, we chose patients with Medicaid, Medicare, and Private insurance labels for analysis, further merging Medicaid and Medicare into the "Public" label, in order to mainly inspect the disparity between people receiving public and private insurance. If a patient is covered by more than one type of health insurance in their lifetime, we chose the health insurance type that inferred the lowest socioeconomic status for the patient (i.e. Medicaid < Medicare < Public). As for the preprocessing of other demographic attributes, the age attribute was separated into three groups: 1-39, 40-49, 50-64. The division points were established to ensure an equitable distribution of patient counts across each group. As for race, we selected the two major ethnic groups in the datasets: White and Black, and the remaining ethnicities were pooled as "Others".

To decrease confounding factors that possibly affect our analysis, we only included 41,571 and 10,220 chest X-ray images in MIMIC-CXR-JPG and CheXpert, respectively, that matched the following three conditions: (1) Patient's age under 65. (2) Image labeled as "no finding" and without "support devices". (3) Frontal view image (including posteroanterior/anteroposterior views). In the first condition, we excluded patients that were automatically covered by the public insurance, and focused our analyses on economically underprivileged patients in the public insurance group; in the second condition, we excluded patients with thoracic diseases to focus on how normal chest X-ray itself conveyed socioeconomic information; in the last condition, only frontal view images were considered to simplify our analyses. We randomly divided our extracted dataset into 0.8/0.1/0.1 splits for training, validation, and testing set, respectively, and ensured that patients in each split set did not overlap.

## 2.2. Models and Metrics

In our study, we utilized three different vision models: DenseNet121 [Huang et al. \(2017\)](#), SwinTransformer

[Liu et al. \(2022\)](#), MedMamba [Yue and Li \(2024\)](#). Each of them represents a specific type of deep vision model. As for further training details, please refer to appendix B. As for health insurance type classifying performance, AUC (area under receiver operating characteristic curve) was utilized as our main metric.

## 3. Experiments

### 3.1. Health Insurance Prediction from CXRs

**Setting** In our first experiment, we have trained and tested our three chosen model: DenseNet121, SwinTransformer, and MedMamba on both MIMIC-CXR-JPG and CheXpert, respectively, to predict the health insurance type of each patient.

**Results** As Table 1 indicates, in MIMIC-CXR-JPG, all trained health insurance predicting models could achieve an AUC performance around 0.65, with MedMamba having the best average AUC (0.6669) on the insurance predicting task and SwinTransformer performed the worst (0.6261). On the other hand, the models trained by on CheXpert also had a better-than-random performance on the health insurance prediction, as the best performance is 0.6761. Notice that CheXpert contains less and smaller sized images compared to MIMIC-CXR-JPG, which may be the major cause of the AUC decrease in SwinTransformer and MedMamba. The result suggested that the models are not simply guessing and that chest X-rays contain certain insurance information for the model to learn from.

Table 1: AUC Performance on Insurance Prediction

	DenseNet	Swin	MedMamba
MIMIC	0.6385	0.6261	0.6669
CheXpert	0.6761	0.6168	0.6188

### 3.2. Localization of insurance information on Xray - Patch-based training

**Setting** We investigated whether insurance information could be localized to a particular anatomical region or image patch with two different approaches. We divided each chest X-ray into 3x3 squared cells of approximately equal size. (Most grids are in size of 150x150, as some grids are sized 148x150 or 148x148 due to indivisible width and height.) We trained a

health insurance classification model based on MedMamba using two different approaches. (1) Remove-One-Patch: Select one of the nine patches, and remove all information from that patch by setting pixel values within the patch to zero. (2) Keep-One-Patch: Select one of the nine patches, and remove all information from the image by setting pixel values to zero except for the pixels within the patch. Visualization of the two approaches are shown in Figure 1. MIMIC-CXR-JPG was chosen as the main dataset for this experiment due to its larger data size.

**Results** Figure 1 reveals the AUC performance on the insurance type prediction task for the Remove-One-Patch and Keep-One-Patch experiment. The lowest performance (0.6332) occurs when we remove the center part of the image, while the highest performance (0.6572) appears when pixels at the mid-lower corner are set to zero. Conversely, the highest performance (0.6541) in Keep-one-patch experiment lands in the top-left corner when it is the only part that is preserved in an image. AUC performance drops to the lowest (0.6063) when only the bottom-right part of the image is retained. While the pulmonary area is located at the middle of a chest radiograph, these results suggest that the health insurance information is not only inferred from lungs. Combining the two experiments, the upper two-third part seems to contain the most health insurance type information, while the bottom part of a chest radiograph contains the least of it.

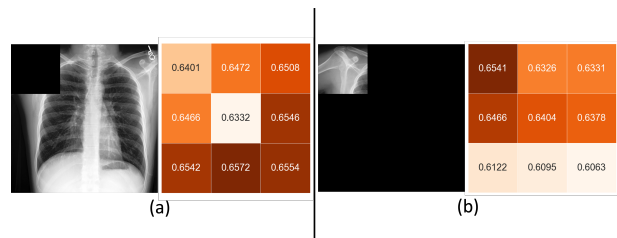


Figure 1: (a) The left image provides an example of the Remove-One-Patch method. The right image shows insurance type prediction AUC when only the corresponding patch area in the 3x3 grid is removed. (b) The left image provides an example of the Keep-One-Patch method. The right image shows insurance type prediction AUC when only the corresponding patch area in the 3x3 grid is retained.

### 3.3. Experiments on Demographic Mediators

**Setting** Based on the premise that deep learning models can effectively discern health insurance types from chest X-ray images, a pertinent inquiry arises: Is the insurance classification directly inferred, or is it mediated through demographic features like age, sex, or race? To answer this, we conducted an insurance detection experiment using other demographics. Specifically, we trained tree-based and clustering machine learning models including Random Forest Breiman (2001), Decision Tree Quinlan (1986), XGBoost Chen and Guestrin (2016), CatBoost Prokhorenkova et al. (2018), and KNN Fix (1985) to predict health insurance type from a combination of demographic attributes: age, sex, and race. The hyperparameter is tuned by GridSearchCV from the Scikit-Learn package. In addition, given the observation that the portion of Black people covered by private insurance is disproportionately lower than that in the White, we also conducted an experiment in which we trained, validated, and tested a health insurance type classifier only on patients that are reported as white. In this part of experiment, MIMIC-CXR-JPG and MedMamba were also chosen as the main dataset and deep vision model.

**Result** Table 2 shows the performance of multiple machine learning models to predict health insurance from the combination of age, race, and sex attributes. Among the five machine learning models (Random Forest, XGBoost, CatBoost, Decision Tree, KNN) that we have evaluated, XGBoost have the highest AUC value, but could only reach 0.5905. Therefore, we concluded that the results do not indicate a strong correlation between health insurance types and the three demographic features, as all the AUCs are no higher than 0.6. Table 3 demonstrates the health insurance type prediction performance of the DenseNet121 model trained solely from White people in our dataset. We observed that the performance is relatively consistent with training our model with the entire dataset, except a noticeable drop DenseNet. In this experiment, we could still observe the superiority of MedMamba over the other two models. Our results indicate that the ability of deep vision models to predict health insurance types is not mediated by race features.

Table 2: Health insurance type prediction performance across multiple machine learning methods given the combination of age, race, and sex attributes.

Model	AUC
Random Forest	0.5527
XGBoost	0.5905
CatBoost	0.5847
KNN	0.5475
Decision Tree	0.5527

Table 3: AUC of DenseNet121 trained on isolated White people in MIMIC-CXR-JPG

DenseNet	Swin	MedMamba
0.6047	0.6290	0.6679

#### 4. Discussion

Despite our results in AI algorithms predicting insurance information from chest X-ray images, there are several limitations in our work. First, we only chose one of the insurance types per person in their lifetime, which ignored the possible socioeconomic transition of a patient. Second, we did not explicitly show that health insurance information biases disease prediction in deep vision training, but since humans could easily learn the association between socioeconomic status and disease distribution, we should assume it being a simple association for a model to learn from. Third, we admit that the hyperparameters may not be best-tuned in the vision models due to computational limits, especially for the suspicious drop in DenseNet performance in isolated White people in MIMIC-CXR-JPG.

Our work serves as a calling to re-examine the current AI models trained on chest X-ray datasets as they may utilize socioeconomic information as shortcut feature for disease diagnosis. Moreover, we are looking forward to actively developing methods that ensure algorithms do not use these shortcut features. Although many features correlated with socioeconomic status may also be legitimate biological markers of a disease, we are aiming for techniques that can disentangle these signals and completely remove

the influence of features that only predict socioeconomic status, while downgrading the contribution of features that are associated with both socioeconomic status and the disease of interest. In this way, we move the field toward developing truly robust and equitable clinical tools, rather than simply creating more powerful versions of biased systems.

#### 5. Conclusion

We demonstrated that the state-of-the-art deep vision models learn health insurance type information from chest X-ray images, and that it is not mediated by common demographic factors. Despite the convenience of AI technology, we should utilize these deep learning models more cautiously when applying them to real-world medical tasks.

#### References

- Jason Adleberg, Amr Wardeh, Florence X Doo, Brett Marinelli, Tessa S Cook, David S Mendelson, and Alexander Kagen. Predicting patient demographics from chest radiographs with deep learning. *Journal of the American College of Radiology*, 19(10):1151–1161, 2022.
- Gebreyowhans H Bahre, Hassan Hamidi, Andrew B Sellergren, Alessandro Quarta, Leo Anthony Celi, Francesco Calimeri, and Laleh Seyyed-Kalantari. Underdiagnosis bias mitigation with expert foundation model’s representation. *IEEE Access*, 2025.
- Imon Banerjee, Kamanasish Bhattacharjee, John L Burns, Hari Trivedi, Saptarshi Purkayastha, Laleh Seyyed-Kalantari, Bhavik N Patel, Rakesh Shiradkar, and Judy Gichoya. “shortcuts” causing bias in radiology artificial intelligence: causes, evaluation, and mitigation. *Journal of the American College of Radiology*, 20(9):842–851, 2023.
- Leo Breiman. Random forests. *Machine learning*, 45(1):5–32, 2001.
- Joy Buolamwini and Timnit Gebru. Gender shades: Intersectional accuracy disparities in commercial gender classification. In *Conference on fairness, accountability and transparency*, pages 77–91. PMLR, 2018.
- Pierre Chambon, Jean-Benoit Delbrouck, Thomas Sounack, Shih-Cheng Huang, Zhihong Chen, Maya

- Varma, Steven QH Truong, Chu The Chuong, and Curtis P Langlotz. Chexpert plus: Augmenting a large chest x-ray dataset with text radiology reports, patient demographics and additional image formats. *arXiv preprint arXiv:2405.19538*, 2024.
- Tianqi Chen and Carlos Guestrin. Xgboost: A scalable tree boosting system. In *Proceedings of the 22nd acm sigkdd international conference on knowledge discovery and data mining*, pages 785–794, 2016.
- Evelyn Fix. *Discriminatory analysis: nonparametric discrimination, consistency properties*, volume 1. USAF school of Aviation Medicine, 1985.
- Robert Geirhos, Jörn-Henrik Jacobsen, Claudio Michaelis, Richard Zemel, Wieland Brendel, Matthias Bethge, and Felix A Wichmann. Shortcut learning in deep neural networks. *Nature Machine Intelligence*, 2(11):665–673, 2020.
- Judy Wawira Gichoya, Imon Banerjee, Ananth Reddy Bhimoreddy, John L Burns, Leo Anthony Celi, Li-Ching Chen, Ramon Correa, Natalie Dullerud, Marzyeh Ghassemi, Shih-Cheng Huang, et al. Ai recognition of patient race in medical imaging: a modelling study. *The Lancet Digital Health*, 4(6):e406–e414, 2022.
- Gao Huang, Zhuang Liu, Laurens Van Der Maaten, and Kilian Q Weinberger. Densely connected convolutional networks. In *Proceedings of the IEEE conference on computer vision and pattern recognition*, pages 4700–4708, 2017.
- Jeremy Irvin, Pranav Rajpurkar, Michael Ko, Yifan Yu, Silviana Ciurea-Ilcus, Chris Chute, Henrik Marklund, Behzad Haghgo, Robyn Ball, Katie Shpanskaya, et al. Chexpert: A large chest radiograph dataset with uncertainty labels and expert comparison. In *Proceedings of the AAAI conference on artificial intelligence*, volume 33, pages 590–597, 2019.
- A Johnson, L Bulgarelli, T Pollard, B Gow, B Moody, S Horng, LA Celi, and R Mark. Mimic-iv (version 3.0). physionet, 2024.
- Alistair Johnson, Matt Lungren, Yifan Peng, Zhiyong Lu, Roger Mark, Seth Berkowitz, and Steven Horng. Mimic-cxr-jpg-chest radiographs with structured labels. *PhysioNet*, 101:215–220, 2019a.
- Alistair EW Johnson, Tom J Pollard, Nathaniel R Greenbaum, Matthew P Lungren, Chih-ying Deng, Yifan Peng, Zhiyong Lu, Roger G Mark, Seth J Berkowitz, and Steven Horng. Mimic-cxr-jpg, a large publicly available database of labeled chest radiographs. *arXiv preprint arXiv:1901.07042*, 2019b.
- Alistair EW Johnson, Lucas Bulgarelli, Lu Shen, Alvin Gayles, Ayad Shammout, Steven Horng, Tom J Pollard, Sicheng Hao, Benjamin Moody, Brian Gow, et al. Mimic-iv, a freely accessible electronic health record dataset. *Scientific data*, 10(1):1, 2023.
- Byungju Kim, Hyunwoo Kim, Kyungsu Kim, Sungjin Kim, and Junmo Kim. Learning not to learn: Training deep neural networks with biased data. In *Proceedings of the IEEE/CVF conference on computer vision and pattern recognition*, pages 9012–9020, 2019.
- Salamata Konate, Léo Lebrat, Rodrigo Santa Cruz, Judy Wawira Gichoya, Brandon Price, Laleh Seyyed-Kalantari, Clinton Fookes, Andrew Bradley, and Olivier Salvado. Interpretability of ai race detection model in medical imaging with saliency methods. *Computational and Structural Biotechnology Journal*, 28:63–70, 2025.
- Charaka Vinayak Kumar, Ashok Uralana, Gopichand Kanumolu, Bala Mallikarjunarao Garlapati, and Pruthwik Mishra. No llm is free from bias: A comprehensive study of bias evaluation in large language models. *arXiv preprint arXiv:2503.11985*, 2025.
- Agostina J Larrazabal, Nicolás Nieto, Victoria Peterson, Diego H Milone, and Enzo Ferrante. Gender imbalance in medical imaging datasets produces biased classifiers for computer-aided diagnosis. *Proceedings of the National Academy of Sciences*, 117(23):12592–12594, 2020.
- Kaizhao Liang, Lizhang Chen, Bo Liu, and Qiang Liu. Cautious optimizers: Improving training with one line of code. *arXiv preprint arXiv:2411.16085*, 2024.
- Ze Liu, Han Hu, Yutong Lin, Zhuliang Yao, Zhenda Xie, Yixuan Wei, Jia Ning, Yue Cao, Zheng Zhang, Li Dong, et al. Swin transformer v2: Scaling up capacity and resolution. In *Proceedings of the*

- IEEE/CVF conference on computer vision and pattern recognition*, pages 12009–12019, 2022.
- Ziad Obermeyer, Brian Powers, Christine Vogeli, and Sendhil Mullainathan. Dissecting racial bias in an algorithm used to manage the health of populations. *Science*, 366(6464):447–453, 2019.
- Liudmila Prokhorenkova, Gleb Gusev, Aleksandr Vorobev, Anna Veronika Dorogush, and Andrey Gulin. Catboost: unbiased boosting with categorical features. *Advances in neural information processing systems*, 31, 2018.
- J. Ross Quinlan. Induction of decision trees. *Machine learning*, 1(1):81–106, 1986.
- Olivier Salvado, Salamata Konate, Rodrigo Santa Cruz, Andrew Bdadley, Judy Wawira Gichoya, Laleh Seyyed-Kalantari, Brandon Price, Clinton Fookes, and Léo Lebrat. Localisation of racial information in chest x-ray for deep learning diagnosis. In *2024 IEEE International Symposium on Biomedical Imaging (ISBI)*, pages 1–4. IEEE, 2024.
- Laleh Seyyed-Kalantari, Guanxiong Liu, Matthew McDermott, Irene Y Chen, and Marzyeh Ghassemi. Chexclusion: Fairness gaps in deep chest x-ray classifiers. In *BIOCOMPUTING 2021: proceedings of the Pacific symposium*, pages 232–243. World Scientific, 2020.
- Laleh Seyyed-Kalantari, Haoran Zhang, Matthew BA McDermott, Irene Y Chen, and Marzyeh Ghassemi. Underdiagnosis bias of artificial intelligence algorithms applied to chest radiographs in underserved patient populations. *Nature medicine*, 27(12):2176–2182, 2021.
- Yubiao Yue and Zhenzhang Li. Medmamba: Vision mamba for medical image classification. *arXiv preprint arXiv:2403.03849*, 2024.
- MIMIC-CXR-JPG [Johnson et al. \(2019a,b\)](#) is an extended image dataset for MIMIC-IV v3.0, including 377,110 chest X-ray images in total.
- On the other hand, CheXpert [Irvin et al. \(2019\)](#) includes 224,316 chest X-rays from 65,240 patients from both in-patient and out-patient centers of Stanford Hospital between October 2002 and July 2017. The recent CheXpert Plus paper [Chambon et al. \(2024\)](#) provides additional demographic information of each patient, including their health insurance type, race, sex, and age.

## Appendix B. Model architecture

DenseNet121 [Huang et al. \(2017\)](#) comprises multiple convolutional neural network layers with denser residual connections than the traditional ResNet, which demonstrates equal importance of density with depth and width of a model. SwinTransformer [Liu et al. \(2022\)](#) is a variant of vision transformer model, where self-attention is performed on shifted image windows. This idea largely decreases the memory complexity and reduces the downsides of separated image areas. In our study, the version of SwinV2-B\* was utilized specifically. Lastly, MedMamba [Yue and Li \(2024\)](#) combines both a convolutional branch and a state-space sequence model branch, Mamba, to utilize the local inductive bias and global feature extraction from each branch. As for the classification, a single linear layer was added after the penultimate layer of DenseNet121, SwinV2-B\* and MedMamba.

All of the experiments utilized Lion [Liang et al. \(2024\)](#) as their optimizer, and the learning rate was 1e-6 for DenseNet, 1e-5 for SwinTransformer and MedMamba. The learning rate of DenseNet was adjusted to 1e-5 in experiment 3.3 for better performance. The batch size was 32 across our experiments, and we did not implement dropout or weight decay for regularization for simplicity. In MIMIC-CXR-JPG, all images were resized to 448x448 otherwise mentioned, while in CheXpert, all images were resized to 320x320 since the original image size in CheXpert is smaller than in MIMIC-CXR-JPG. All images were preprocessed with RandomHorizontalFlip, RandomRotation and Normalization in PyTorch for augmentation. A cross-entropy loss was utilized for health insurance type classification tasks. We trained our model on the training dataset, and selected the weights by the best performing average area under receiver operating characteristic curve (AUC) on the validation dataset. The final perfor-

## Appendix A. Dataset description

MIMIC-IV v3.0 [Johnson et al. \(2024, 2023\)](#) is a large medical dataset containing over 265,000 patients’ data collected at Beth Israel Deaconess Medical Center in Boston, MA, in the intensive care unit or emergency department between 2008-2022, while

mance was tested on the testing dataset with the chosen weights. All experiments were trained on a single NVIDIA GeForce RTX 3090 or RTX 6000 Ada GPU.